

An Interpretable Hybrid Predictive Model of COVID-19 Cases using Autoregressive Model and LSTM

Yangyi Zhang*

Sui Tang *[†]

Guo Yu *[‡]

September 19th, 2022

Abstract

The Coronavirus Disease 2019 (COVID-19) has posed a severe threat to global human health and economic. It is an urgent task to build reliable data-driven prediction models for Covid 19 cases to improve public policy making. However, COVID-19 data shows special transmission characteristics such as significant fluctuations and non-stationarity, which may be difficult to be captured by a single predictive model and poses grand challenges in effective forecasting. In this paper, we proposed a novel Hybrid data-driven model combining Autoregressive model (AR) and long short-term memory neural networks (LSTM). It can be viewed as a new neural network model and the contribution of AR and LSTM is auto tuned in the training procedure. We conduct extensive numerical experiments on data collected from 8 counties of California that display various trends. The numerical results show the Hybrid model' advantages over AR and LSTM by its predictive powers. We show that the Hybrid model achieved 4.195% MAPE, outperformed the AR 5.629% and LSTM 5.070% on average, and provide a discussion on interpretability.

1 Introduction

The coronavirus disease 2019 (COVID-19) pandemic has posed a severe threat to global human health and economics while producing some of the richest data we have ever seen in terms of infectious disease tracking. The quantity and quality of data placed epidemic modelling and forecasting at the forefront of worldwide public policy making. Compared to previous infectious diseases, COVID-19 shows special transmission characteristics, yielding significant fluctuations and non-stationarity in the new COVID-19 cases. This poses grand challenges in effective forecasting, and, on the other hand, draws attention of the global community to epidemic tracking and forecasting.

In the last three years, various models and methods have been developed to forecast COVID-19 cases (see survey in [14] and references therein). These models can be roughly grouped into two categories: mechanistic models and data-driven models. The mechanistic models aim at directly characterizing the underlying mechanisms of COVID-19

*Department of Mathematics, University of California Santa Barbara. Email: yangyi@ucsb.edu;

[†]Department of Mathematics, University of California Santa Barbara. Email: suitang@ucsb.edu;

[‡]Department of Statistics and Applied Probability, University of California Santa Barbara. Email: guoyu@ucsb.edu; [◊]: Corresponding authors

transmission. Typical examples of mechanistic models are based on differential equations, such as the compartmental models SIR and SEIR [5, 22, 23, 26]. The data-driven models formulate the prediction of the COVID-19 cases primarily as a regression problem and exploit fully data-adaptive approaches to understand the functional relationship between COVID-19 cases with a set of observable variables. Data-driven models include classical statistical models such as Autoregressive models (AR) [17, 18, 28] and Support Vector Regression (SVR) [12, 29, 30], and deep learning models [1, 7, 9, 13, 16, 25, 32]. In this paper, we will focus on data-driven models.

Autoregressive models express the response variable as a linear function of its previous observations, and enjoy simple structure and strong interpretability. Furthermore, AR models are found to be powerful in capturing short-term changing trends in the time series. However, they may fail to capture the highly nonlinear patterns caused by long-term effects in the dynamics. In contrast, deep learning models have been well-examined in their ability to learn complex patterns, but they are short of interpretability due to its black-box nature. This lack of interpretability prevents people from drawing useful conclusions from the model outputs, and thus hinders effective policy making [20]. This observation motivates us to consider a Hybrid model that additively combines the two types of models and tries to possess the advantages of each one.

Specifically, we consider the Hybrid modeling of COVID-19 data using AR and LSTM (Long Short Term Memory Neural Network). AR [6] is a popular tool in time series analysis, with numerous applications in various application fields, including infectious disease modelling [3, 19]. For the neural network part, we consider LSTM [24] for its impressive power in capturing complex dependence structures in sequential data. LSTM has been used to achieve the best-known results for many problems on sequential data. We build a Hybrid model that **additively combines** LSTM and AR and examine its performance on COVID-19 case prediction in California counties. In this paper, we collect and consider data from 8 counties in California. But our model is applicable to other time series forecasting tasks. All codes are accessible through links on the reference page [34]. A long-term mission is to stretch the application of Hybrid models beyond COVID-19 forecasting: toward other fast-moving epidemics and cases that require accurate prediction and interpretability.

1.1 Significance of Proposed Research.

Modeling and forecasting the spread of COVID-19 is an important yet challenging task. We propose a Hybrid model, that outperforms the neural networks yet enjoys the interpretability of linear models. The analysis of the cumulative and new number of COVID-19 cases helps to predict its prevalence trends, and to inform policy makers to improve pandemic planning, resource allocation, and implementation of social distancing measures and other interventions. We tailor data analysis for California counties, thus to help local government to provide a more accurate reference for the prediction and early warning of infectious diseases.

Although in this paper we focus on confirmed cases prediction, we note that the proposed framework can be easily extended to tackle other COVID-19 or more general epidemiological tasks (e.g., hot spot prediction). Furthermore, the proposed method has its own research significance from a methodological perspective. For example, it raised the open

questions on studying its theoretical guarantees, mathematical quantification of prediction, and interpretability.

1.2 Related work

Using combination of different models has proven to be an effective way of improving empirical predictions in various applications. One can refer to the Hybrid modelling of other types of infectious disease in [2, 4, 31, 35, 36] and sunspot monitoring [33]. The idea using an additive combination of AR model (or more generally, ARIMA model) with LSTM has recently appeared in [10, 11] for time series forecasting with applications in gas and oil well production and sunspot monitoring.

We note a significant difference with previous methods: our approach include a different data-processing procedure and trains the two components in the model jointly, while previous Hybrid modeling techniques take a sequential approach to training. Specifically, previous methods first perform filtering using AR or did a prior decomposition for AR and LSTM part before modeling the counterpart. For example, in [10], the preprocessed data is used to fit an ARIMA model first before the residual term is used as the input to train a LSTM model. In contrast, we design a general network architecture that includes both AR part and LSTM part additively and jointly trains the whole architecture by minimizing the empirical risk. By doing so, we do not arbitrarily give preference to any of the two additive components. Instead, the relative weights of the interpretable AR part and the predictive LSTM part are determined fully by data.

2 Data

We study the number of daily COVID-19 cases in 8 California counties: Los Angeles, San Diego, San Francisco, Santa Barbara, Fresno, Sacramento, Ventura, and Riverside, from 2020-02-01 to 2022-09-05. These data can be found on the official website of California State Government [8]. Specifically, we collect data from the statewide COVID-19 cases deaths tests. Since there is only one missing value, collected in Los Angeles, we drop the observations of the same date from all counties' data. The final dataset contains consecutive time series data, collected from the 8 California counties, each with 948 observations collected in the past three years. We will use Y_t to denote the number of COVID-19 cases at time t , where t is an integer index that takes value in $\{1, 2, \dots, 948\}$.

3 Methods

In this section, we first briefly overview the two building blocks of our additive Hybrid model, namely the AR and the LSTM, and their relative advantages. Then we present our Hybrid model which combines these two building blocks additively, and we intuitively elaborate why it is better than the two individual components.

3.1 AutoRegressive (AR) Model

In time-series, we often observe similarities between past and present values. For example, by knowing the price of a stock in the past few days, we can often make a rough prediction about its value tomorrow. AR is a simple model that utilized this empirical observation and can yield very accurate prediction in applications. It represents the time series values

using linear combination of the past values. The number of past values used is called the lag number and often denoted by p . Mathematically, let ϵ_t denote the Gaussian noise at time t with mean 0 and variance σ^2 . The structure equation of AR(p) model can be represented as

$$Y_t = a_0 + a_1Y_{t-1} + a_2Y_{t-2} + \cdots + a_pY_{t-p} + \epsilon_t \quad (1)$$

where a_0 is the intercept, and a_1, \dots, a_p represent the coefficients. AR model is often effective on stationary data. To ensure stationarity, a common trick is to apply the differencing operation on the time series. A time series value at time t that has been differenced once, $Y^{(1)}$, is defined as follows:

$$Y_t^{(1)} = Y_t - Y_{t-1}, \quad (2)$$

and higher order differencing operation can be defined recursively. However, an AR model is not sufficient to capture the non-linear dependence structure, which is found to be an important feature of the COVID-19 data, indicated by Figure 4.1. A purely AR based model is thus insufficient for the task of COVID-19 cases prediction.

3.2 Long Short Term Memory Network (LSTM)

RNN (Recurrent Neural Network), different from traditional neural networks, is able to utilize previous knowledge to predict future ones. However, it suffers from the long term dependency problem: as the network grows larger through time, the gradient decays quickly during back propagation, making it impossible to train RNN models with long unfolding in time. To solve this problem, Hochreiter and Schmidhuber (1997) introduced a special type of RNN called LSTM with a proper gradient-based learning algorithm [24].

We employ a LSTM regression model, which is represented as

$$Y_t = G_\theta(Y_{t-1}, \dots, Y_{t-p}), \quad (3)$$

where we use Y_{t-1}, \dots, Y_{t-p} as the sequential input data; G represents the neural network architecture shown in Figure 1 and θ represents the weight parameters in neural networks.



Figure 1: This diagram illustrates the architecture of a simple LSTM network for regression. The network starts with a sequence input layer followed by an LSTM layer. The network ends with a fully connected layer and a regression output layer.

An LSTM layer consists of several cells. The core concepts of a LSTM cell are the cell states and its various gates, see Figure 2. The cell state C_{t-1} at time step $t - 1$ acts as a transport highway that transfers relative information all the way down the sequence chain, which intuitively characterizes the "memory" of the network. The cell states, in

principle, carry relevant information throughout the processing of the sequence. So even information from the earlier time steps can make its way to later time steps, reducing the effects of short-term memory. The Forget Gate decides what information should be kept. The Input Gate decides what information is to be added from the current step and update the cell state C_t at time step t . The Output Gate determines what the next hidden state h_t should be. The four gates comprise a fully connected feed forward neural network.

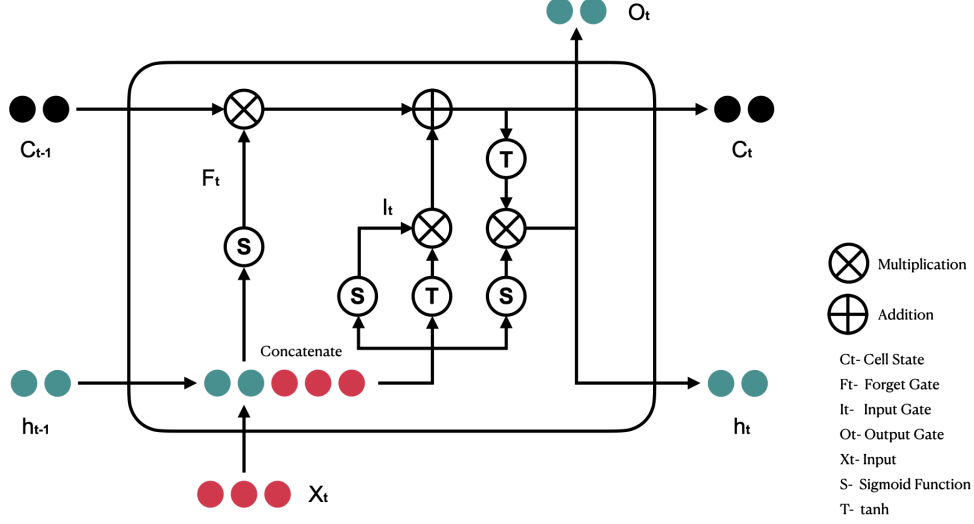


Figure 2: Structure of a LSTM cell that describes the cell state c_t (green circles, $\dim = 2$) and hidden state h_t (red circles, $\dim = 2$) and various gates [15].

To achieve optimal prediction results using LSTM model, it is crucial to have a careful hyperparameter tuning, including the choice of units (dimension of the hidden state), the number of cells (i.e. the number of time steps), and layers. This is usually a difficult task in practice. For example, few LSTM cells are unlikely to capture the structure of the sequence, while too many LSTM cells might lead to overfitting.

However, just like other neural networks, a well-known limitation of LSTM is its lack of interpretability [20].

3.3 The Hybrid Model

As discussed above, both AR and LSTM have their relative strength and limitations in their prospective domains. To conserve the advantages and overcome the limitations, we combine the two models additively into one single Hybrid model, which is expressed as

$$Y_t = \alpha \text{AR}(p) + (1 - \alpha) G_\theta(Y_{t-1}, \dots, Y_{t-p}), \quad (4)$$

where p is the lag number and α weights the contribution of two components: by tuning the value of α , one can strike a balance between the prediction given by AR and LSTM parts, and thus a prediction of linear and nonlinear signals.

The addition as a combination method is preferable since it preserves the low complexity and enjoys a better interpretability than other methods do, for example, the one by multiplication. We will compare the performance of the Hybrid model to its two separated

components.

We illustrate the structure of the Hybrid model. By intuition, the AR component would capture the linear relationship in time series and the LSTM component would describe the nonlinear patterns. In Section 4, we show how to train the weights in each of the two components in a fully data-adaptive manner by minimizing the empirical risk. We will compare the contribution of the Hybrid model’s AR component and LSTM component in Section 5.

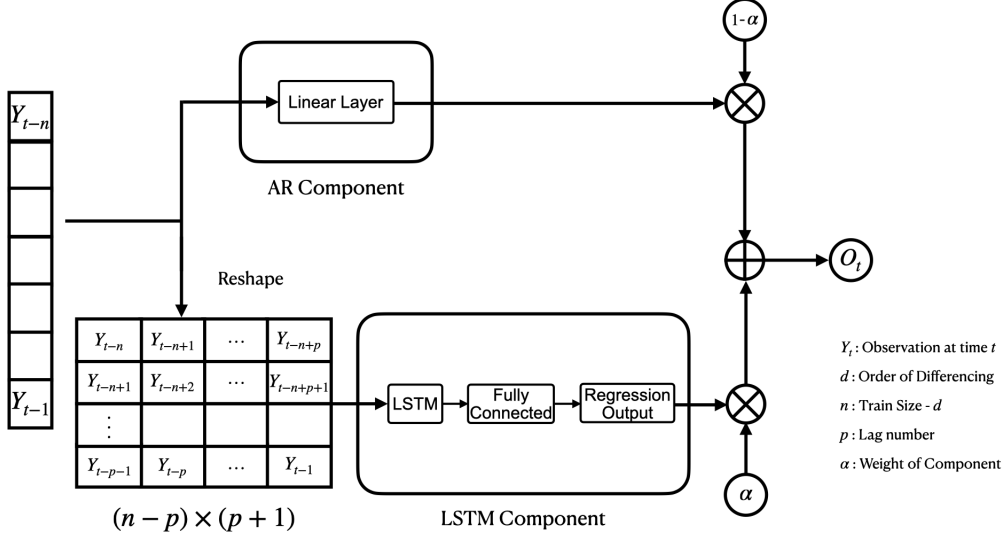


Figure 3: Visualization of the Hybrid method.

4 Training

In this section, we provide details on how we fit the models discussed in Section 3, and introduce the experiment setups for performance evaluation.

4.1 Data Preprocessing and Preparation

Smoothing. Recall that we denote Y_t as the number of COVID-19 cases at time t . We adopt the standard smoothing techniques below to smooth out the irregular roughness between time steps:

$$\bar{Y}_t := \frac{1}{\tau} \left(\sum_{i=t-\tau+1}^t Y_i \right),$$

where τ is the smoothing lag number. In our study, we choose $\tau = 7$ by exploiting the day of week effect: the number of observations each date is influenced by which day of a week it is. For example, the observations of COVID-19 case detection are empirically higher on Fridays, which might be attributed to the fact that people have time to do the testing on Fridays. The day of week effect has long been observed in healthcare and the stock market. To avoid the day of week effect, we smoothed the data by using the average of observations from 6 previous dates and the current date. We will use the smoothed data as the ground truth throughout the study.

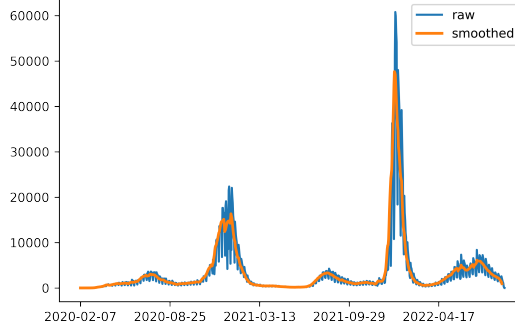


Figure 4: An example of visualizing daily observations, where blue line represents the data before smoothing, orange line represents data after smoothing. The data is collected from the Los Angeles county.

4.2 Experiment setup for single trial

In reality, we often aim at making reliable and timely predictions based on an appropriate length of data. Furthermore, it is well-known that the different variants of COVID-19 could result in different transmission mechanisms, leading the joint distribution of confirmed cases to shift from time to time. Therefore, it is not advised to train the model using all historical data since pandemic. Therefore, we cut the time series into different pieces and split each piece into training set and test set. We then apply the model training and testing on each piece, which we call a trial. For each trial, we do a three-step data preprocessing:

Differencing: Statistical methods such as AR have guaranteed performance on stationary time series. However, the raw data are typically not stationary. Differencing can help us stabilize the mean of a time series by removing changes in the level of a time series, and therefore eliminating (or reducing) trend and seasonality. This can make the differenced time series stationary. Specifically, we keep differencing data until stationarity is achieved by standard tests such as Augmented Dickey Fuller Unit Root Test (ADF) [21] or Kwiatkowski Phillips Schmidt Shin Test (KPSS) [27]. We found a consistent stationarity among different trials with only one differencing operation, as indicated in Figure 6.

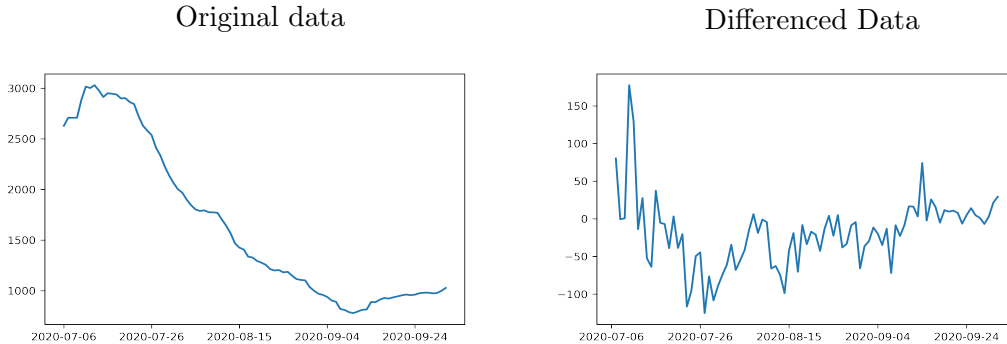


Figure 5: The left panel shows the smoothed data, which would be used as the real observations in this study. The right panel shows the smoothed data after 1st order differencing. The original data is not stationary, indicated by the two tests mentioned above, and the differenced data is stationary.

Rescale. After differencing the data, we rescale the training data into the $[-1, 1]$ with:

$$Y_{\text{train,scaled}} = \frac{Y_{\text{train}} - \mu_{\text{train}}}{Y_{\text{max,train}} - Y_{\text{min,train}}}$$

where μ_{train} denotes the mean of Y_{train} , $Y_{\text{max,train}}$ denotes the maximum of Y_{train} , $Y_{\text{min,train}}$ denotes the minimum of Y_{train} , and $Y_{\text{train,scaled}}$ denotes training data after scaling. We also apply the same re-scaling map to the testing data:

$$Y_{\text{test,scaled}} = \frac{Y_{\text{test}} - \mu_{\text{train}}}{Y_{\text{max,train}} - Y_{\text{min,train}}}$$

Thus the testing data does not affect the selection of our scalar. We train the model on $Y_{\text{train,scaled}}$ and make predictions with $Y_{\text{test,scaled}}$. Finally, we apply the inverse rescaling map to retrieve the original scale, and thus make comparison with the original data.

Reshaping. After differencing and rescaling the data, we transform the data into supervised learning form as shown below in the table 1.

	Input	Output
Row 1	$[Y_{t-n}, \dots, Y_{t-n+1}]$	Y_{t-n+p}
Row 2	$[Y_{t-n+1}, \dots, Y_{t-n+2}]$	$Y_{t-n+p+1}$
Row 3	$[Y_{t-n+2}, \dots, Y_{t-n+3}]$	$Y_{t-n+p+2}$
\vdots	\vdots	\vdots

Table 1: The input-output data format. Here p is the lag number.

This step is also conducted on the testing data for all three models and the training data for the LSTM model and the Hybrid model.

We are now ready to conduct the experiment on a single trial. To begin with, each trial has 88 continuous observations. We apply a first order differencing to make the trial data stationary, at the cost of losing one observation. Now we have 87 observations. The first 62 would be used as the training data: notice that our training size is 63, since the 62 differenced values are derived from 63 observations. The remaining 25 values will be used to make a testing data matrix.

We apply the rescaling on the training and test data. Then we reshape the testing data of length 25 to a matrix of size $(18, 8)$. For each of the 18 rows, the first 7 values are model inputs, which would return a single predicted value to us: an prediction for the rescaled $Y_t^{(1)}$, where the superscript 1 refers to the first order differencing as defined in (2). Let us denote this prediction with:

$$\hat{Y}_{t,\text{scaled}}^{(1)} \tag{5}$$

We derive an prediction of the ground truth Y_t from (5). First, we scale (5) back to the original scale by applying the inverse function of rescaling to it. Then (5) becomes an prediction of $Y_t^{(1)}$, say $\hat{Y}_t^{(1)}$. We now retrieve an estimation of the ground truth Y_t with:

$$\hat{Y}_t = \hat{Y}_t^{(1)} + Y_{t-1} \tag{6}$$

Notice that all observations before Y_t are known. Since we obtain one estimation from each row, we will end up with a list of 18 estimated values. We assess the model by comparing these 18 estimations with the 18 corresponding ground truth values.

4.3 Choice of Hyper-parameters

In this section, we detail how we choose the hyper-parameters for each predictive model.

AR: We used lag number 7 for the sake of interpretability, since 7 is the number of days in a week. There could exist more scientific methods to select the lag number. For example, we may check the Bayesian information criterion (BIC). BIC is a class of information criteria to measure the goodness of fit of a statistical model. It builds on the concept of entropy and can weigh the complexity of the estimated model against the goodness of fit of this model to the data. This information helps to assess the model’s parameters and how well the model performed.

LSTM: We use batch number 1, epoch number 100, and units 1. The neural network is trained on mean square error, with optimizer adam. The fully connected layer (in Figure 1) is activated by the default linear function. Since the performance is well enough for our purpose, we do not tune the model further.

Hybrid Model: This neural network is the addition of 2 layers: an AR layer and a LSTM layer, after being weighted by a trainable coefficient between 0 and 1. We use the same set of hyperparameters as we do in the AR model and the LSTM model. As a result, we have some flexibility to tune to make the performance better.

5 Results

The results include three sections: Model Evaluations, Prediction, and Interpretability. In Model Evaluations, we introduce the metrics we use to evaluate the models and on which we compare the models’ performances. In the Prediction, we exhibit the visualizations of several interesting trials and compare the numerical predictions and evaluations of the three models. In the Interpretability part, we compare the AR component of the Hybrid model with the AR model. This is to examine how we may interpret the Hybrid model.

5.1 Model Evaluations

Evaluation metric. We use a quantitative measure to evaluate and compare the performance of models: the Mean Absolute Percentage Error (MAPE), with formulas provided below:

$$\text{MAPE} = \frac{100}{n} \sum_{t=1}^n \frac{|\hat{Y}_t - Y_{\text{true},t}|}{|Y_{\text{true},t}|} \quad (7)$$

We use this relative error as the data size vary largely and it is more reasonable to consider the relative error. A model is desirable when values of MAPE are close to 0.

We examine the performance of all 3 models on different time periods within the available range. This is essential in our research, since the performance of a model is not constant on different trends; by intuition, a model performs better on smooth curves than it does on steep curves. By repeating our evaluation process on different time periods thus different trends, we wish to learn on what trends do the model give the best performance. Such understanding will help us decide to what degrees we may trust the performance

of the models. Another reason for the repetition is that, while the AR method yields the same model with the same piece of data, the LSTM and the Hybrid method do not. We evaluate the models repeatedly to reduce the influence brought by the instability of model training.

For the repetition, we choose a step number of 7: we leave 7 days between the first date of any two consecutive training sets. Although a larger number of repetitions seems desirable, increasing the repetition number is at the cost of making neighboring training sets closer to each other. However, the difference in performance between two neighboring training sets, that are too close to each other, would be attributed more to the instability of model training than to the difference in trend. Such results give us little information about the model performance over trend. In the end, we let the step number be the same as our lag number. By doing so, we assume the concept of a week is important in forecasting.

5.2 Prediction

In this section, we present the visual and numerical results for all three models. We perform a comprehensive comparison of the performance for three models on various situations and multiple counties, showing the advantage of the Hybrid model. All predictions are transformed back to the original scale.

5.2.1 Visualizations

We compare the three models' performance on COVID cast forecasting in 8 counties of California. For each county, we test the models' performance on several different situations: for example, when the training data has an up trend and the testing data has a down trend. From all trials we practiced, we choose the following trials as representatives of different combinations of training and testing data, since they reflect the general model performances well.

Case 1. Curved Training Data and Down Trend Testing Data

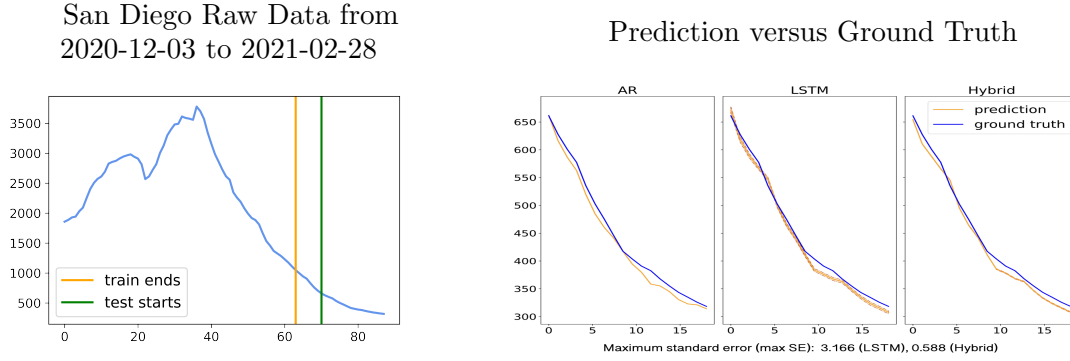


Figure 6: The left panels show the training and testing data. The right panels show the ground truth versus forecasts of the AR, LSTM, and Hybrid model, respectively. We display the average prediction (solid line) with 2 times standard error (shaded region). The standard error across 100 runs are reported for LSTM and Hybrid. MAPE from left to right: 2.523%, 2.692%, 2.419%

Case 2. Up Trend Training and Down Trend Testing

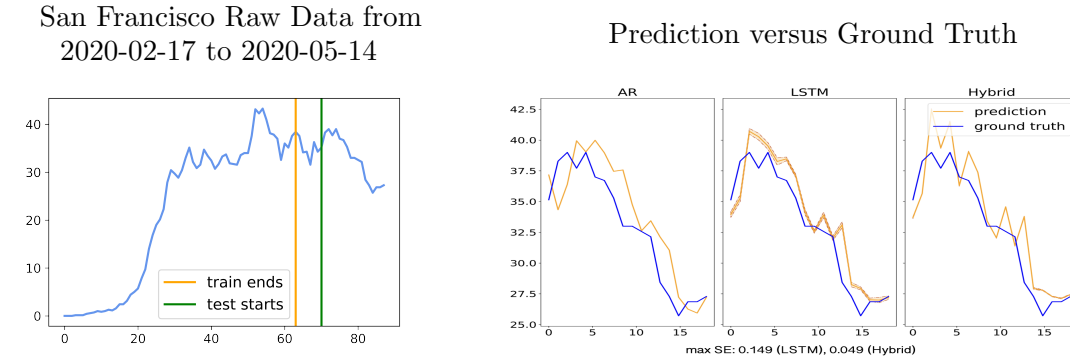


Figure 7: The left panels show the training and testing data. The right panels show the ground truth versus forecasts of the AR, LSTM, and Hybrid model, respectively. We display the average prediction (solid line) with 2 times standard error (shaded region). The standard error across 100 runs are reported for LSTM and Hybrid. MAPE from left to right: 6.174%, 4.469%, 4.993%

Case 3. Up Trend Training and Up Trend Testing

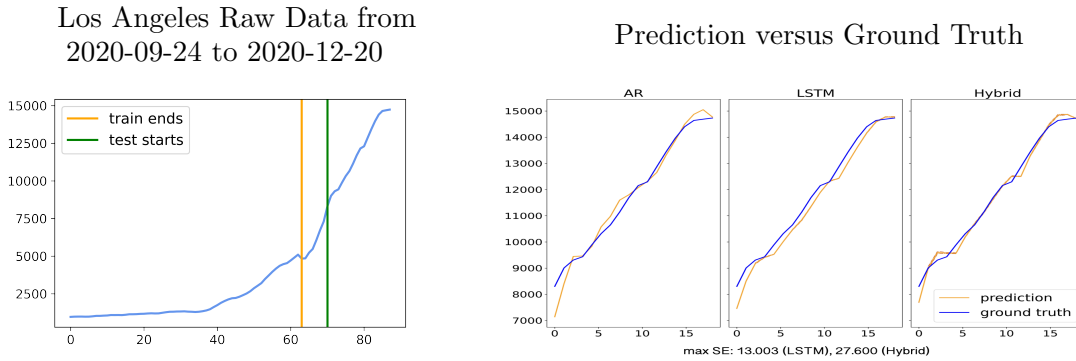
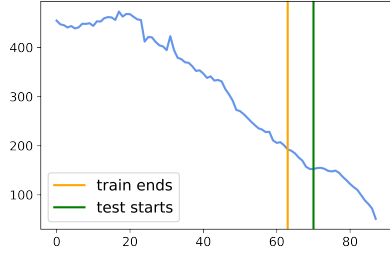


Figure 8: The left panels show the training and testing data. The right panels show the ground truth versus forecasts of the AR, LSTM, and Hybrid model, respectively. We display the average prediction (solid line) with 2 times standard error (shaded region). The standard error across 100 runs are reported for LSTM and Hybrid. MAPE from left to right: 2.368%, 2.541%, 1.647%

Case 4. Down Trend Training and Down Trend Testing

San Francisco Raw Data from
2022-06-10 to 2022-09-05



Prediction versus Ground Truth

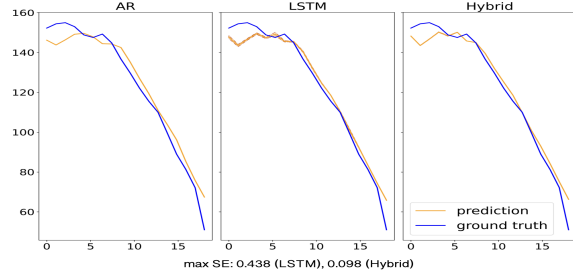
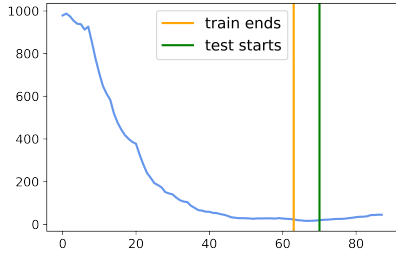


Figure 9: The left panels show the training and testing data. The right panels show the ground truth versus forecasts of the AR, LSTM, and Hybrid model, respectively. We display the average prediction (solid line) with 2 times standard error (shaded region). The standard error across 100 runs are reported for LSTM and Hybrid. MAPE from left to right: 5.251%, 4.105%, 4.116%

Case 5. Down Trend Training and Up Trend Testing

Santa Barbara Raw Data from
2022-01-17 to 2022-04-14



Prediction versus Ground Truth

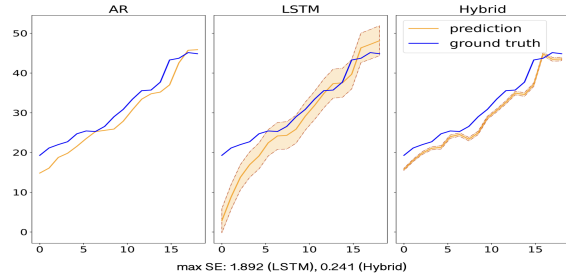
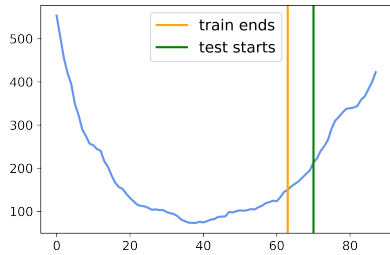


Figure 10: The left panels show the training and testing data. The right panels show the ground truth versus forecasts of the AR, LSTM, and Hybrid model, respectively. We display the average prediction (solid line) with 2 times standard error (shaded region). The standard error across 100 runs are reported for LSTM and Hybrid. MAPE from left to right: 9.061%, 21.137%, 8.978%

Riverside Raw Data from
2022-02-16 to 2022-05-14



Prediction versus Ground Truth

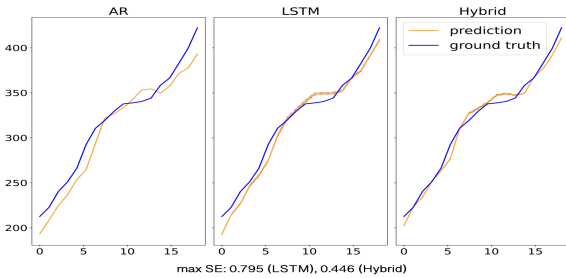


Figure 11: The left panels show the training and testing data. The right panels show the ground truth versus forecasts of the AR, LSTM, and Hybrid model, respectively. We display the average prediction (solid line) with 2 times standard error (shaded region). The standard error across 100 runs are reported for LSTM and Hybrid. MAPE from left to right: 4.356%, 2.898%, 1.922%

Case 6. Jagged Testing

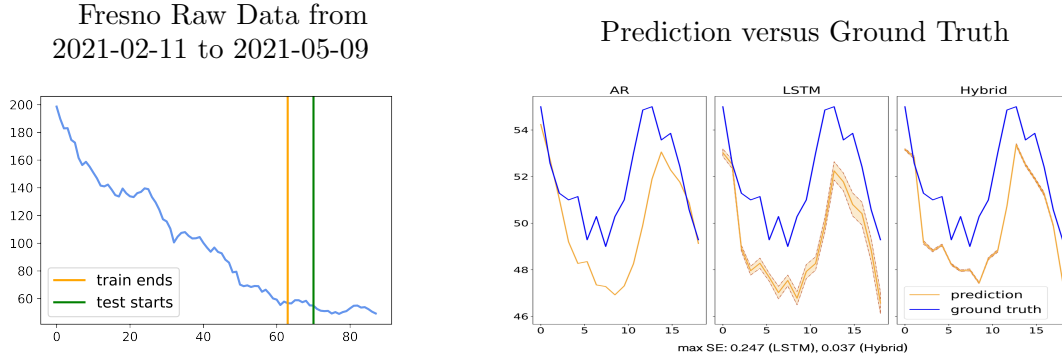


Figure 12: The left panels show the training and testing data. The right panels show the ground truth versus forecasts of the AR, LSTM, and Hybrid model, respectively. We display the average prediction (solid line) with 2 times standard error (shaded region). The standard error across 100 runs are reported for LSTM and Hybrid. MAPE from left to right: 3.675%, 5.049%, 3.718%

To ensure the results above are representative, we run each trial above 100 times, visualize the mean and standard error of these trials, and present maximum standard error and averaged MAPE. The Hybrid model is more stable than the LSTM. While AR outperforms LSTM on some cases, the Hybrid model outperforms both in most cases, except that in Case 2 and in Case 6. The MAPE, averaged on the 100 trials, shows that LSTM (4.469%) outperforms Hybrid (4.993%) slightly in Case 2. However, as shown in the right panel of Figure 7, the Hybrid model captures the general trend of ground truth better than LSTM does. Similarly, in Case 6, AR (3.675%) outperforms Hybrid (3.718%) slightly. Yet, as shown in the right panel of Figure 12, the Hybrid model captures the general trend of ground truth better than AR does.

Beside, interestingly enough, the Hybrid model always seem to capture the ground truth's trend. Actually, the shape of Hybrid's forecasts resembles either that of the AR model or that of the LSTM model, or it resembles a combination of both. When AR model captures the trend better than the LSTM does, the Hybrid model resembles the AR model in forecast shape: for example, in Case 2, San Francisco 2020-02-17 to 2020-05-14, and in Case 5, Santa Barbara 2022-01-17 to 2022-04-14. When LSTM model captures the trend better than the AR does, the Hybrid model resembles the LSTM model in forecast shape: for example, in Case 4, San Francisco 2022-06-10 to 2022-09-05, and in Case 5, Riverside 2022-02-16 to 2022-12-20. On jagged testing data, where AR performs better on some part and LSTM better on the other, the Hybrid model presents advantages of both models: for example, in Case 6, Figure 12, the Hybrid model resembles AR on the two ends, where AR performs better, and it resembles LSTM in shape between day 5 to day 15, where LSTM seems to capture the trend better.

5.2.2 General Performance

After looking at the representative trials in 5.2.1, we evaluated the model performances numerically, on the 8 California counties and multiple trials, with the method we explained in 4, Model Evaluations. The results are given in Table 2.

County	AR	LSTM	LSTM (Double)	Hybrid
Los Angeles	5.153 (1.071)	5.202 (1.409)	6.073 (1.591)	3.391 (0.622)
San Diego	4.446 (0.652)	3.983 (1.071)	5.249 (1.606)	3.302 (0.651)
San Francisco	4.754 (0.421)	4.194 (0.518)	5.647 (1.239)	3.671 (0.401)
Santa Barbara	7.706 (1.714)	6.046 (0.994)	7.345 (1.785)	6.117 (1.352)
Fresno	6.549 (1.668)	5.595 (1.387)	7.100 (2.125)	4.277 (0.735)
Sacramento	5.240 (0.787)	4.838 (0.787)	4.986 (0.721)	3.888 (0.691)
Ventura	6.525 (0.706)	5.910 (1.231)	6.840 (1.947)	5.001 (0.917)
Riverside	5.660 (0.925)	4.794 (0.769)	6.403 (1.724)	3.913 (0.683)

Table 2: MAPE (by percentage) for each model on each county, averaged on all trials. The inconsistent performances of neural networks have been compensated by the small step value, which is 7. The value in parenthesis is the standard deviation.

From the result above, we can see the Hybrid model outperforms the AR model and the LSTM models stably: it generally yield the smallest average MAPE. To be specific, the general MAPE of each model (AR, LSTM, LSTM with 2 layers, and Hybrid), averaged on the results for all 8 counties, is 5.629%, 5.070%, 6.205%, and 4.195% in order. In general, the Hybrid model has the best general performance, and it outperforms the AR model by approximately 1.5%. The LSTM model suffers from overfitting when a second LSTM layer is added.

Besides, as shown in 5.1.1 Visualizations, the Hybrid model captures general forecasting trend more stably than the other two models do: it always take the shape of the component model that captures trend better.

5.2.3 Performance on latest data

We also checked the model performances for the same 8 counties on the latest trial, from 2022-06-10 to 2022-09-05, thus to provide some insights on the timely prediction of our models.

County	AR	LSTM	LSTM (Double)	Hybrid
Los Angeles	4.221	3.754 (0.112)	3.546 (0.160)	3.348 (0.032)
San Diego	3.749	3.476 (0.035)	3.554 (0.126)	3.328 (0.020)
San Francisco	5.251	4.097 (0.067)	4.115 (0.084)	4.136 (0.026)
Santa Barbara	4.731	4.143 (0.030)	4.139 (0.089)	4.164 (0.012)
Fresno	3.475	3.114 (0.076)	3.394 (0.149)	2.942 (0.009)
Sacramento	4.685	3.831 (0.053)	3.743 (0.076)	3.888 (0.023)
Ventura	4.143	3.563 (0.028)	3.487 (0.057)	3.418 (0.018)
Riverside	4.752	3.419 (0.088)	3.304 (0.147)	3.203 (0.041)

Table 3: MAPE (by percentage) for each model on each county, on the latest trial, from 2022-06-10 to 2022-09-05. The results for LSTM and Hybrid are each averaged on 100 runs, to compensate the inconsistent performances of neural networks. The value in parenthesis is the standard deviation. AR has 0 or small standard deviation for the same trial. The Hybrid model is usually the best in performance and has the lowest standard deviation.

Notice-worthily, the AR model takes much smaller amount of time to train. While it takes approximately 0.1 time unit to train an AR model, it takes approximately 10 time unit to train a LSTM model or a Hybrid model. There is no significant difference between training time of LSTM and Hybrid, possibly because they are different by only an AR layer, which is relatively fast to train.

5.3 Interpretability

In this section, we study how AR and LSTM components contribute to the Hybrid model when fitting the data. Our purpose is to seek the insights into explaining why the Hybrid model enjoys the better performance in general. And more importantly, we seek to use the interpretation from the fitted Hybrid model to provide practical guidance to the public health policy making process.

Note that all models are trained on the normalized data as described in Section 4. Consequently all figures below report predictions on the normalized scales.

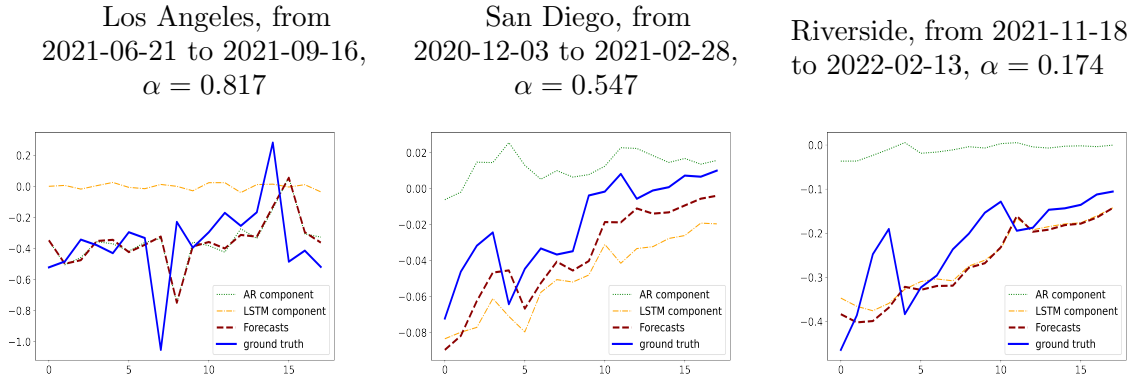


Figure 13: The forecasts of a Hybrid model versus the ground truth, and the contribution of its AR and its LSTM component.

In Figure 13, we present three settings with different signal strength ratio (represented by the value of α) of the AR components and LSTM components in the prediction of the Hybrid model. Specifically, the larger value of α indicates the AR component dominates the LSTM component in prediction, and the smaller value of α indicates otherwise. We found that the component that has stronger signal characterizes the general trend in the data while the other helps to stabilize the variance. This observation sheds light into why the Hybrid model provides better predictive performance in general than a single model.

Moreover, the fitted value of α provides a characterization of the intrinsic nonlinearity of the data, and consequently the difficulty of exploiting interpretation in the linear components of the fitted Hybrid model. The smaller the value of α , the higher weight the nonlinear fit using LSTM has in the final prediction. In such a setting, coefficients in the AR components should be given less weight into generating interpretation for policy making. Equivalently, for larger value of α , it is more trustworthy to derive coefficients interpretation from the important AR part. This observation is helpful for public policy maker to distinguish among different virus transmission stages.

Models	intercept	Y_{t-1}	Y_{t-2}	Y_{t-3}	Y_{t-4}	Y_{t-5}	Y_{t-6}	Y_{t-7}
AR	-0.106	-0.124	0.108	0.063	0.183	0.001	0.039	0.654
Hybrid	-0.008	0.702	0.142	0.044	0.210	0.089	0.114	-0.108

Table 4: Coefficients of AR model v.s. AR coefficients of Hybrid model. The AR component dominates the prediction ($\alpha = 0.817$). MAPE for AR and Hybrid: 3.088%, 2.593%

Models	intercept	Y_{t-1}	Y_{t-2}	Y_{t-3}	Y_{t-4}	Y_{t-5}	Y_{t-6}	Y_{t-7}
AR	-0.000	-0.019	0.061	-0.077	0.117	-0.041	0.165	0.553
Hybrid	0.022	0.478	-0.298	0.080	-0.003	-0.169	0.049	-0.243

Table 5: Coefficients of AR model v.s. AR coefficients of Hybrid model. The AR and the LSTM components have similar weight in prediction ($\alpha = 0.547$). MAPE for AR and Hybrid: 2.523%, 1.950%

Models	intercept	Y_{t-1}	Y_{t-2}	Y_{t-3}	Y_{t-4}	Y_{t-5}	Y_{t-6}	Y_{t-7}
AR	-0.046	0.103	-0.166	0.145	-0.168	0.311	-0.170	0.813
Hybrid	0.025	0.680	0.043	-0.079	-0.138	0.080	-0.156	-0.063

Table 6: Coefficients of AR model v.s. AR coefficients of Hybrid model. The LSTM component dominates the prediction ($\alpha = 0.174$). MAPE for AR and Hybrid: 9.337%, 4.665%

Finally, we observe interesting patterns of the coefficients estimates in the AR components of the Hybrid model compared with the coefficients in the pure AR model. As shown in Table 4 to Table 6, across the three settings of different values of α , the pure AR model tends to put heavier weight in coefficients of larger lags, say Y_{t-7} . In contrast, the AR component in the Hybrid model tends to focus on capturing the short history, i.e., the coefficients associated with smaller lags (e.g., Y_{t-1}) tend to have larger estimates. This indicates that the short history pattern in the data could be well approximated by a simple (say, linear) model, while the longer history in the data possesses more complicated nonlinear structure that requires a LSTM component to fit.

6 Conclusion

In this paper we introduce a novel Hybrid model that borrow strength from a highly structured Autoregressive model and a LSTM model for the task of Covid-19 cases prediction. Through intensive numerical experiments, we conclude that the Hybrid model yields more desirable predictive performance than considering the AR or the LSTM counterpart alone. In principle, the Hybrid model enjoy the advantages of each of its two building blocks: the expressive power of LSTM in representing nonlinear patterns in the data and the interpretability from the simple structures in AR. Consequently, the proposed Hybrid model is useful in simultaneously providing accurate prediction and shedding light into understanding the transition of the virus transmission phases, thus providing guidance to the public health policy making process.

It is also noteworthy that the predictive performance of the proposed Hybrid model can be further improved by properly choosing the hyperparameters. Furthermore, while we considered LSTM as the nonlinear component in the Hybrid model, it can be substituted by any other deep learning models.

7 Acknowledgement

Y.Zhang was partially supported by Raymond L Wilder Award sponsored by University of California Santa Barbara and Hellman Family Faculty Fellowship. S.T. was partially supported by Regents Junior Faculty fellowship, Faculty Early Career Acceleration grant sponsored by University of California Santa Barbara, Hellman Family Faculty Fellowship and the NSF DMS-2111303. G.Y. was partially supported by Regents Junior Faculty fellowship, Faculty Early Career Acceleration grant sponsored by University of California Santa Barbara.

References

- [1] Madini O Alassafi, Mutasem Jarrah, and Reem Alotaibi. Time series predicting of covid-19 based on deep learning. *Neurocomputing*, 468:335–344, 2022.
- [2] Maher Ala’raj, Munir Majdalawieh, and Nishara Nizamuddin. Modeling and forecasting of covid-19 using a hybrid dynamic model based on seird with arima corrections. *Infectious Disease Modelling*, 6:98–111, 2021.
- [3] R Allard. Use of time-series analysis in infectious disease surveillance. *Bulletin of the World Health Organization*, 76(4), 1998.
- [4] Adeboye Azeez, Davies Obaromi, Akinwumi Odeyemi, James Ndege, and Ruffin Muntabayi. Seasonality and trend forecasting of tuberculosis prevalence data in eastern cape, south africa, using a hybrid model. *International Journal of Environmental Research and Public Health*, 13(8), 2016.
- [5] Andrea L Bertozzi, Elisa Franco, George Mohler, Martin B Short, and Daniel Sledge. The challenges of modeling and forecasting the spread of covid-19. *Proceedings of the National Academy of Sciences*, 117(29):16732–16738, 2020.
- [6] George EP Box, Gwilym M Jenkins, Gregory C Reinsel, and Greta M Ljung. *Time series analysis: forecasting and control*. John Wiley & Sons, 2015.
- [7] Vinay Kumar Reddy Chimmula and Lei Zhang. Time series forecasting of covid-19 transmission in canada using lstm networks. *Chaos, Solitons & Fractals*, 135:109864, 2020.
- [8] CHHS Open Data. Statewide covid-19 cases deaths tests, September 6th 2022.
- [9] Mohammad Reza Davahli, Krzysztof Fiok, Waldemar Karwowski, Awad M. Aljuaid, and Redha Taiar. Predicting the dynamics of the covid-19 pandemic in the united states using graph theory-based neural networks. *International Journal of Environmental Research and Public Health*, 18(7), 2021.
- [10] Dongyan Fan, Hai Sun, Jun Yao, Kai Zhang, Xia Yan, and Zhixue Sun. Well production forecasting based on arima-lstm model considering manual operations. *Energy*, 220:119708, 2021.

- [11] Oussama Fathi. Time series forecasting using a hybrid arima and lstm model. *Velvet Consulting*, pages 1–7, 2019.
- [12] Soham Guhathakurata, Souvik Kundu, Arpita Chakraborty, and Jyoti Sekhar Banerjee. 18 - a novel approach to predict covid-19 using support vector machine. In Utku Kose, Deepak Gupta, Victor Hugo C. de Albuquerque, and Ashish Khanna, editors, *Data Science for COVID-19*, pages 351–364. Academic Press, 2021.
- [13] Mohamed Hawas. Generated time-series prediction data of covid-19’s daily infections in brazil by using recurrent neural networks. *Data in brief*, 32:106175, 2020.
- [14] Amir H. Gandomi Iman Rahimi, Fang Chen. A review on covid-19 forecasting models. *Neural Computing and Applications*, February 4th 2021.
- [15] Raimi Karim. Animated rnn, lstm and gru, July 4th 2020.
- [16] Jie Long, AQM Khaliq, and Khaled M Furati. Identification and prediction of time-varying parameters of covid-19 model: a data-driven deep learning approach. *International Journal of Computer Mathematics*, 98(8):1617–1632, 2021.
- [17] Mohsen Maleki, Mohammad Reza Mahmoudi, Darren Wraith, and Kim-Hung Pho. Time series modelling to forecast the confirmed and recovered cases of covid-19. *Travel Medicine and Infectious Disease*, 37:101742, 2020.
- [18] Daniel J McDonald, Jacob Bien, Alden Green, Addison J Hu, Nat DeFries, Sangwon Hyun, Natalia L Oliveira, James Sharpnack, Jingjing Tang, Robert Tibshirani, et al. Can auxiliary indicators improve covid-19 forecasting and hotspot prediction? *Proceedings of the National Academy of Sciences*, 118(51):e2111453118, 2021.
- [19] Nicholas G. Reich Michael A. Johansson, John S. Brownstein Aditi Hota, and Mauricio Santillana. Evaluating the performance of infectious disease forecasts: A comparison of climate-driven and seasonal dengue forecasts for mexico. *scientific reports*, 2016.
- [20] W. James Murdoch, Chandan Singh, Karl Kumbier, Reza Abbasi-Asl, and Bin Yu. Definitions, methods, and applications in interpretable machine learning. *Proceedings of the National Academy of Sciences*, 116(44):22071–22080, oct 2019.
- [21] Rizwan Mushtaq. Testing time series data for stationarity. *SSRN*, August 2011.
- [22] Faïçal Ndaïrou, Iván Area, Juan J Nieto, and Delfim FM Torres. Mathematical modeling of covid-19 transmission dynamics with a case study of wuhan. *Chaos, Solitons & Fractals*, 135:109846, 2020.
- [23] Eamon B O’Dea and John M Drake. A semi-parametric, state-space compartmental model with time-dependent parameters for forecasting covid-19 cases, hospitalizations and deaths. *Journal of the Royal Society Interface*, 19(187):20210702, 2022.
- [24] Jürgen Schmidhuber Sepp Hochreiter. Long short-term memory. *Neural Computation*, 9(8):1735–1780, 1997.
- [25] Farah Shahid, Aneela Zameer, and Muhammad Muneeb. Predictions for covid-19 with deep learning models of lstm, gru and bi-lstm. *Chaos, Solitons & Fractals*, 140:110212, 2020.

- [26] Kehui Sun Shaobo He, Yuexi Peng. Seir modeling of the covid-19 and its dynamics. *Nonlinear Dynamics*, 101, June 18th 2020.
- [27] Yongcheol Shin and Peter Schmidt. The kpss stationarity test as a unit root test. *Economics Letters*, 38(4):387–392, 1992.
- [28] Arash Sioofy Khoojine, Mahdi Shadabfar, Vahid Reza Hosseini, and Hadi Kordestani. Network autoregressive model for the prediction of covid-19 considering the disease interaction in neighboring countries. *Entropy*, 23(10):1267, 2021.
- [29] Dimple Tiwari, Bhoopesh Singh Bhati, Fadi Al-Turjman, and Bharti Nagpal. Pandemic coronavirus disease (covid-19): World effects analysis and prediction using machine-learning techniques. *Expert Systems*, 39(3):e12714, 2022.
- [30] Milind Yadav, Murukessan Perumal, and M Srinivas. Analysis on novel coronavirus (covid-19) using machine learning methods. *Chaos, Solitons & Fractals*, 139:110050, 2020.
- [31] Weirong Yan, Yong Xu, Xiaobing Yang, and Yikai Zhou. A hybrid model for short-term bacillary dysentery prediction in yichang city, china. *Japanese Journal of Infectious Diseases*, 63(4):264–270, 2010.
- [32] Abdelhafid Zeroual, Fouzi Harrou, Abdelkader Dairi, and Ying Sun. Deep learning methods for forecasting covid-19 time-series data: A comparative study. *Chaos, Solitons & Fractals*, 140:110121, 2020.
- [33] G.Peter Zhang. Time series forecasting using a hybrid arima and neural network model. *Neurocomputing*, 50:159–175, 2003.
- [34] Yangyi Zhang. <https://github.com/yangyi-zhang/covid-forecasting>, 2022.
- [35] Weiping Zhao, Yunpeng Chen, Ying Li, and Weimin Guan. Prediction of covid-19 data using hybrid modelling approaches. *Frontiers in public health*, page 1795, 2022.
- [36] Nanning Zheng, Shaoyi Du, Jianji Wang, He Zhang, Wenting Cui, Zijian Kang, Tao Yang, Bin Lou, Yuting Chi, Hong Long, et al. Predicting covid-19 in china using hybrid ai model. *IEEE transactions on cybernetics*, 50(7):2891–2904, 2020.